

A Novel Mixed-Integer Linear Programming Formulation for Continuous-Time Inventory Routing

Akang Wang^{1,2}, Xiandong Li¹, Jeffrey E. Arbogast³, Zachary Wilson³, and
Chrysanthos E. Gounaris^{*1}

¹Department of Chemical Engineering and Center for Advanced Process Decision-making, Carnegie Mellon
University, Pittsburgh, PA 15213, USA

²Shenzhen Research Institute of Big Data, Shenzhen, Guangdong, China

³Air Liquide, Newark, DE 19702, USA

Abstract

Inventory management, vehicle routing, and delivery scheduling decisions are simultaneously considered in the context of the inventory routing problem. This paper focuses on the continuous-time version of this problem where, unlike its more traditional discrete-time counterpart, the distributor is required to guarantee that inventory levels are maintained within the desired intervals at any moment of the planning horizon. In this work, we develop a compact mixed-integer linear programming formulation to model the continuous-time inventory routing problem. We further discuss means to expedite its solution process, including the adaptation of well-known rounded capacity inequalities to tighten the formulation in the context of a branch-and-cut algorithm. Through extensive computational studies on a suite of 90 benchmark instances from the literature, we show that our branch-and-cut algorithm outperforms the state-of-the-art approach. We also consider a new set of 63 instances adapted from a real-life dataset and show our algorithm's practical value in solving instances with up to 20 customers to guaranteed optimality.

Keywords: continuous-time inventory routing, inventory management, vehicle routing, branch-and-cut, rounded capacity inequalities

*Corresponding author: gounaris@cmu.edu

1 Introduction

The Inventory Routing Problem (IRP) integrates inventory management, vehicle routing, and delivery scheduling decisions, whereby delivery quantities are at the discretion of the distributor and are to be co-optimized with delivery routes. The IRP most often arises in the context of *vendor-managed inventory* (Yao et al., 2007), where a supplier monitors inventory levels at customers and makes the replenishment decisions for products delivered to customers. This is often a win-win strategy for both suppliers and customers: suppliers can coordinate shipment made to customers so as to save distribution costs, while customers can benefit from avoiding efforts for explicit inventory control. The integration of inventory control and delivery planning is ubiquitously practiced in industry. For example, the industrial gases company Air Liquide has recently pointed out that its business model is transitioning from customer-managed inventory to vendor-managed inventory, which necessitates inventory routing optimization techniques (Arbogast and Kontopoulos, 2017). To this end, the ROADEF/EURO Challenge 2016 (ROADEF, 2016) was based on the real-life experience of Air Liquide. Indeed, developing optimization techniques for inventory routing is of great interest for both academic research and industrial applications.

There are many IRP variants and they can be distinguished based on different categories. The first category is the inventory replenishment policy. Replenishment policies define pre-established rules to be imposed on the quantity delivered to a customer in each visit, with the *order-up-to-level* and the *maximum-level* policies being most common. The former calls for filling the inventory to the tank capacity whenever a customer is replenished (Archetti et al., 2007), while the latter allows for flexible replenishment and only requires that tank capacities are respected (Desaulniers et al., 2015; Avella et al., 2017). Clearly, the maximum-level policy provides more flexibility for replenishment decisions and is thus more preferable from a cost-saving perspective. The second category is the objective function. Traditionally, the objective of an IRP is to minimize the total cost, including inventory cost and routing cost (Archetti et al., 2007; Desaulniers et al., 2015; Avella et al., 2017). Recently, some research efforts (Archetti et al., 2017; Baldacci et al., 2020; Singh et al., 2015; Kheiri, 2020; Absi et al., 2020; He et al., 2020; Su et al., 2020) have been focused on minimizing the so-called “logistic ratio”, which is the ratio of the total cost to the amount of product distributed. Assessing the efficiency of a distribution policy through measures that consider both the distribution cost and the amount of product distributed is in fact a common industrial practice,

but unfortunately, choosing the ratio function as an objective results in a fractional programming model (Radzik, 2013), which is usually much harder to solve. Interested readers are referred to the work of Coelho et al. (2013) for a comprehensive review on the IRP and its variants.

A new dimension to categorize the IRP is whether to discretize the planning horizon. The discrete-time IRP first discretizes a given planning horizon into multiple time periods. It then assumes that customers receive their deliveries at the beginning of each period and can use them to fulfill their demands in that period (Desaulniers et al., 2015), irrespectively of when the actual deliveries take place as a consequence of the specific routing decisions made in each period. In this case, one only enforces inventory constraints at the beginning/end of each time period. In contrast, the continuous-time IRP (CIRP) explicitly accounts for the time it takes to distribute product by vehicles and manages inventory in continuous time, requiring that inventory constraints are satisfied at any time point throughout the planning horizon (Lagos et al., 2020). The practical significance of this depends of course on the exact application, but it can be argued that it is imperative in settings where feasibility of material storage and timeliness of material transfer are critical. This can be the case in the storage of fuels, chemicals, hazardous materials and regulated substances, among other examples. In these cases, vehicle arrival/departure times at customers cannot be neglected but should be explicitly accounted for by the model, in order for the latter to retain awareness of inventory levels at all times and lead to decisions that enforce them continuously.

The IRP is notoriously hard because three types of decisions have to be made simultaneously: (i) when to serve a given customer, (ii) how much to deliver to a given customer in light of other deliveries, and (iii) how to combine customers into vehicle routes. In the literature, the discrete-time IRP has been extensively studied. The work of Coelho et al. (2012) considered the multi-vehicle IRP with and without consistency requirements, and applied an adaptive large neighborhood search scheme in which some subproblems are solved exactly as mixed-integer linear programs. The first exact algorithm for IRP is from the work of Archetti et al. (2007) in which the authors considered a single-vehicle IRP and proposed a branch-and-cut approach that could solve to optimality benchmark instances with up to 50 customers and 3 time periods. The work of Coelho and Laporte (2013) and Coelho and Laporte (2014) extended the branch-and-cut approach from Archetti et al. (2007) to the multi-vehicle IRP and enhanced it with new valid inequalities. Their algorithm obtained improved upper and lower bounds for many IRP instances. One of the most successful exact

approaches for solving the discrete-time IRP was presented in Desaulniers et al. (2015), where the authors proposed a sophisticated branch-price-and-cut algorithm, solving benchmark instances with up to 50 customers and up to 5 vehicles optimally. In more recent work Avella et al. (2017), single-period tightening cuts called the “disjoint route inequalities” were proposed and incorporated into a branch-and-cut algorithm, resulting in a significant reduction in optimality gaps.

Despite its significance, the CIRP has received very little attention in the literature. The work of Dong et al. (2017) considered the IRP with driver rest constraints and decomposed it into an upper-level routing problem and a lower-level continuous-time scheduling problem. An iterative approach based on the upper and lower levels was then proposed to identify the optimal routing and scheduling design. Fokkema et al. (2020) focused on the supply-driven cyclic CIRP in which inventory is held in containers that act as both storage and a movable transport unit, in the application of biogas transportation. The authors proposed a tour-based formulation that could optimally solve instances with up to 7 customers. The authors of Agra et al. (2022) proposed a location-event model and a vehicle-event model for a single-vehicle CIRP with pickup and delivery, comparing these two models on maritime transportation instances. Another approach was put forth in the work of Lagos et al. (2020). The authors first proved that, when the CIRP instance data includes only rational numbers, there exists a sufficiently fine time discretization such that both routing and inventory replenishment decisions made in the optimal solution will always happen at these discretized time points. Based on this theory, the authors then proposed a *dynamic discretization discovery* algorithm: (i) the planning horizon is first discretized with different resolutions; (ii) for each discretization, after rounding up and down the adjusted travel times, two mixed-integer linear programs are formulated to produce an upper bound and a lower bound, respectively; (iii) if the difference between the two bounds is below a pre-specified tolerance, then the optimality of the CIRP is achieved. The novelty in the dynamic discretization discovery approach is that it identifies exactly which times are needed to obtain an optimal, continuous-time solution by solving a sequence of relatively easy mixed-integer linear programs. The authors generated 90 benchmark instances with up to 15 customers and conducted extensive computational studies that solved 26 of them to optimality. Lagos et al. (2022) applied this discretization approach for addressing a CIRP with out-and-back routes where only a single customer is served in every vehicle route. Clearly, the CIRP is significantly more challenging than the discrete-time IRP, because vehicle routing and

inventory management become much more intertwined.

In this work, we consider the CIRP as defined in Lagos et al. (2020): (i) the maximum-level inventory replenishment policy is adopted; (ii) the objective is to minimize the total routing cost; (iii) inventory levels are monitored and controlled continuously. This CIRP has several complicated characteristics. First, the planning horizon becomes a single but relatively long time period and, thus, vehicles have to be allowed to perform multiple trips. Second, a customer’s total product consumption across the whole planning horizon may exceed the tank capacity, necessitating multiple visits to replenish this customer during this horizon. Last, both vehicle routing designs and delivery scheduling decisions are now constraining the inventory control space, since they are all taken into account explicitly in continuous time.

Although the branch-price-and-cut approach proposed by Desaulniers et al. (2015) was quite successful in solving the discrete-time IRP, it cannot be easily extended to the CIRP due to complications from having to model features like continuous arrival/departure times, multiple vehicle trips and multiple customer visits, among others. Even formulating the CIRP as a mixed-integer linear program is not a straightforward extension from the discrete-time case. To bridge this gap, we propose in this work a novel mixed-integer linear programming (MILP) formulation to model the continuous-time inventory routing problem. This formulation is based on the concept of duplicating customer nodes and arcs to represent routing features like multiple visits at a customer and multiple trips by a vehicle, respectively. We model the vehicle arrival/departure times at customers as continuous variables and manage stock levels in continuous time via appropriately defined inventory balance equations. We also adapt the well-known *rounded capacity inequalities* to strengthen linear programming relaxations in the context of a branch-and-cut solution process. To elucidate the computational competitiveness of our proposed approach compared to the previous state-of-the-art, we conduct extensive studies based on 90 benchmark instances from the literature. Our algorithm could solve 56 of them to optimality within a reasonable amount of time and return a small residual gap for the remaining ones. We further evaluate our algorithm on newly generated benchmark instances that are inspired by realistic data from the ROADEF/EURO Challenge 2016 (ROADEF, 2016). Out of 63 such instances, our branch-and-cut algorithm solved 56 of them to optimality, including a few 20-customer instances that constitute the largest-sized CIRP instances that have been solved to proven optimality in the open literature to-date.

The remainder of the paper is organized as follows. A formal problem definition is given in Section 2. In Section 3, we present the novel MILP formulation to model the CIRP, and then in Section 4 we present opportunities to tighten this model and expedite its solution process. Section 5 presents our computational studies in detail, while we conclude our work with some final remarks in Section 6.

2 Problem Definition

The CIRP is defined over a planning horizon is $H \in \mathbb{R}_{>0}$ and on a directed graph $G = (V, E)$, where $V := \{0\} \cup V_c$ denotes the set of nodes to include a set of customers $V_c := \{1, 2, \dots, n\}$ and the depot (node 0), and $E := \{(i, j) : i \in V, j \in V \setminus \{i\}\}$ is the set of arcs. We assume that the depot has unlimited supply of product. Each customer $i \in V_c$ consumes said product at a constant rate r_i . Additionally, associated with each customer $i \in V_c$ are product inventory levels $I_i^0, I_i^\ell, I_i^u, I_i^H$ to denote respectively the inventory at the beginning of the planning horizon, the lower and upper bounds that should be satisfied throughout the planning horizon, and the lowest acceptable inventory level at the end of the planning horizon. Without loss of generality, we assume that each customer has to be visited at least once, i.e., $I_i^H + r_i H - I_i^0 > 0$ for all $i \in V_c$.

A fleet of K identical vehicles of capacity Q , initially located at the depot, will be used to deliver product to customers so that inventory levels at customers are maintained within the desired intervals. Vehicles are allowed to perform multiple trips and customers are allowed to be visited multiple times during the planning horizon. Loading at the depot and unloading at customers are considered to be instantaneous. However, a vehicle is allowed to remain at a customer location to dispense additional product before proceeding with the next leg of its trip.

Associated with each arc $(i, j) \in E$ are the time t_{ij} and the cost c_{ij} for a vehicle to traverse the arc. Here, we assume that both the travel time and travel cost matrices satisfy the triangle inequality. Furthermore, we do not allow multiple vehicles to visit a customer at the same time. Hence, while a vehicle remains at a customer to perform additional fulfillment, no other vehicle is allowed to visit this customer (other vehicles must wait until the customer becomes available).

We do not consider inventory holding costs at the depot or at customers; hence, the total cost of a route depends only on the vehicle travel cost. The problem's objective is then to identify the minimum-cost routing plan and schedule such that (i) inventory constraints are satisfied; (ii) vehicle

capacities are respected in each trip; (iii) every used vehicle returns to the depot by the end of the planning horizon.

3 Mathematical Modeling

In this section, we present a mathematical formulation for the CIRP. We highlight that the CIRP setting deviates from archetypal vehicle routing problems in a number of non-straightforward ways, posing certain challenges for the modeler. For example, in the CIRP: (i) we need to handle multiple visits at a customer in continuous time; (ii) a vehicle might deliver product multiple times while on a given customer visit; (iii) a vehicle might have to perform multiple trips during the planning horizon; (iv) we need to monitor and constrain inventory levels continuously in time. In what follows, we discuss how to tackle these rich features in our CIRP model.

First, we introduce some notation. During the planning horizon, every customer consumes product at a fixed rate and the total consumption by a customer may exceed the vehicle capacity Q . In such a case, several deliveries must be made to the customer by one or more vehicles. To that end, we will assume that customer $i \in V_c$ can be visited at most n_i times during the planning horizon. Although primarily done for modeling convenience, we note that this assumption also has a practical motivation. Customers are generally not willing to be visited too frequently within a given interval of time. At the same time, a distributor usually sets a minimal amount of product per delivery, and hence, this amount can be utilized to compute a valid value for n_i . Let us define $N_i := \{1, 2, \dots, n_i\}$ to be the set of possible visits to customer $i \in V_c$; for convenience, we also define $N_0 := \{1\}$. Each node of the CIRP network is thus represented by a pair (i, α) , where $i \in V$ indicates either the depot or a customer and $\alpha \in N_i$ indicates the visit number to i . In the case of the depot, the defined “number 1” visit is taken to apply on all occasions when a vehicle returns to the depot, whether it is for replenishment or to conclude its routing assignment. Let (i, α, j, β) represent the arc from node (i, α) to node (j, β) in the network. The idea of duplicating nodes to represent multiple visits at a customer has also been employed in other vehicle routing settings, such as in maritime inventory routing (Agra et al., 2018), periodic vehicle routing (Rothenbächer, 2019), and green vehicle routing (Koyuncu and Yavuz, 2019).

In order to handle multiple trips by a vehicle, we propose a concept called “mode” to indicate arc copies. Let $D := \{0, 1\}$ denote the set of two modes. In mode “0”, a vehicle is considered

to traverse an arc from (i, α) to (j, β) directly, while in mode “1”, it starts from node (i, α) , makes a detour to the depot $(0, 1)$ for replenishment, and then goes to node (j, β) for delivery. We remark that a similar idea was also applied in the work of Karaoglan (2015), in which the authors duplicated the arcs so as to represent the detour trip to the depot while solving the *multi-trip vehicle routing problem*. Let A^d represent the set of valid arcs in mode $d \in D$. In particular, $A^0 := \{(i, \alpha, j, \beta) : i \in V, \alpha \in N_i, j \in V \setminus \{i\}, \beta \in N_j\}$ and $A^1 := \{(i, \alpha, j, \beta) : i, j \in V_c, \alpha \in N_i, \beta \in N_j\} \setminus \{(i, \alpha, i, \beta) : i \in V_c, \alpha, \beta \in N_i, \alpha \geq \beta\}$. Note how, in mode “1”, the arcs (i, α, i, β) with $\alpha < \beta$ are valid, representing cases where a vehicle departs from a customer, returns to the depot for replenishment, and then visits the same customer for delivery again. Let also $\delta_d^+(j, \beta) := \{(i, \alpha) : (i, \alpha, j, \beta) \in A^d\}$ and $\delta_d^-(j, \beta) := \{(i, \alpha) : (j, \beta, i, \alpha) \in A^d\}$ denote the set of nodes in the network that are connected with node (j, β) by in-coming and out-going arcs in mode $d \in D$, respectively.

Objective Function. The objective is to minimize the total travel cost. The cost of traversing an arc from node (i, α) to node (j, β) by a vehicle in mode d is denoted by c_{ij}^d . Clearly, $c_{ij}^0 := c_{ij}$ (direct travel), while $c_{ij}^1 := c_{i0} + c_{0j}$ because the vehicle makes a detour to the depot. Let $x_{i\alpha j\beta}^d$ be a binary variable that is equal to 1, if the arc from (i, α) to (j, β) is traversed in mode d , and 0 otherwise. The objective function is thus defined as

$$\min \sum_{d \in D} \sum_{(i, \alpha, j, \beta) \in A^d} c_{ij}^d x_{i\alpha j\beta}^d. \quad (1)$$

Degree Constraints. Let $y_{j\beta}$ be a binary variable that is equal to 1, if node (j, β) is visited during the planning horizon, and 0 otherwise. If a visit is made to node (j, β) , there must be an arc entering this node and an arc leaving it, as shown by (4) and (5).

$$x_{i\alpha j\beta}^d \in \{0, 1\} \quad \forall (i, \alpha, j, \beta) \in A^d, \forall d \in D \quad (2)$$

$$y_{j\beta} \in \{0, 1\} \quad \forall \beta \in N_j, \forall j \in V_c \quad (3)$$

$$\sum_{d \in D} \sum_{(i, \alpha) \in \delta_d^+(j, \beta)} x_{i\alpha j\beta}^d = y_{j\beta} \quad \forall \beta \in N_j, \forall j \in V_c \quad (4)$$

$$\sum_{d \in D} \sum_{(i, \alpha) \in \delta_d^-(j, \beta)} x_{j\beta i\alpha}^d = y_{j\beta} \quad \forall \beta \in N_j, \forall j \in V_c \quad (5)$$

Fleet Size. The number of used vehicles is bounded from above by K , the size of the fleet (initially located at the depot), as per constraint (6). Note how the number of used vehicles can be expressed

as the number of arcs that leave the depot, i.e., node $(0, 1)$, as there is no detour that starts from the depot.

$$\sum_{(j,\beta) \in \delta_0^-(0,1)} x_{01j\beta}^0 \leq K \quad (6)$$

Route Timing. Let $[W_{j\beta}^\ell, W_{j\beta}^u]$ denote the time window during which a vehicle may arrive at each customer $j \in V_c$ for the β^{th} visit, where $\beta \in N_j$. For now, one may trivially consider the interval between the earliest and latest possible arrival times, independently of the visit number β , i.e., $[W_{j\beta}^\ell, W_{j\beta}^u] := [t_{0j}, H - t_{j0}]$ for all $\beta \in N_j$, noting that tighter values will be proposed later (see Section 4). Obviously, any applicable time windows provided directly as input data can be used instead, if tighter.

Let non-negative variables $a_{j\beta}$ and $d_{j\beta}$ respectively denote the arrival and departure time at node (j, β) , if it is visited. Let also $\tilde{a}_{i\alpha j\beta}$ be an auxiliary non-negative variable to represent the arrival time from node (i, α) to node (j, β) , if this arc is traversed in any mode, and 0 otherwise. Constraints (10)–(12) then enforce that any vehicle can only leave the depot after time 0 and has to return back to the depot by the end of the planning horizon, H . Constraints (13) build the relationship between variables $\tilde{a}_{i\alpha j\beta}$, $a_{j\beta}$ and $d_{j\beta}$. Note that, since the unloading process is instantaneous, the departure from node (j, β) can occur as soon as the arrival itself. The time for traversing an arc from node (i, α) to node (j, β) by a vehicle in mode d is denoted by T_{ij}^d . Clearly, $T_{ij}^0 := t_{ij}$ and $T_{ij}^1 := t_{i0} + t_{0j}$. Constraints (14) relate the departure time at node (i, α) to the arrival time at some node (j, β) when a vehicle travels from (i, α) to (j, β) in either mode 0 or 1. Note how these constraints are in the form of inequalities, allowing for the possibility for a vehicle to slow down while traversing an arc, or equivalently, wait near the customer premises before eventually arriving. We also remark that, even though loading and unloading products are considered to be instantaneous, fixed service times for these operations can be easily taken into

account by modifying constraints (13) and (14) accordingly.

$$a_{j\beta} \in \mathbb{R}_+ \quad \beta \in N_j, \forall j \in V_c \quad (7)$$

$$d_{j\beta} \in \mathbb{R}_+ \quad \beta \in N_j, \forall j \in V_c \quad (8)$$

$$\tilde{a}_{i\alpha j\beta} \in \mathbb{R}_+ \quad \forall (i, \alpha, j, \beta) \in \cup_{d \in D} A^d : i, j \in V_c \quad (9)$$

$$W_{j\beta}^\ell x_{01j\beta}^0 \leq \tilde{a}_{01j\beta} \leq W_{j\beta}^u x_{01j\beta}^0 \quad \forall (j, \beta) \in \delta_0^-(0, 1) \quad (10)$$

$$\tilde{a}_{i\alpha 01} \leq H x_{i\alpha 01}^0 \quad \forall (i, \alpha) \in \delta_0^+(0, 1) \quad (11)$$

$$\tilde{a}_{i\alpha j\beta} \leq W_{j\beta}^u \sum_{\substack{d \in D: \\ (i, \alpha, j, \beta) \in A^d}} x_{i\alpha j\beta}^d \quad \forall (i, \alpha, j, \beta) \in \cup_{d \in D} A^d : i, j \in V_c \quad (12)$$

$$\sum_{(i, \alpha) \in \cup_{d \in D} \delta_d^+(j, \beta)} \tilde{a}_{i\alpha j\beta} = a_{j\beta} \leq d_{j\beta} \quad \forall \beta \in N_j, \forall j \in V_c \quad (13)$$

$$d_{i\alpha} + \sum_{d \in D} \sum_{(j, \beta) \in \delta_d^-(i, \alpha)} T_{ij}^d x_{i\alpha j\beta}^d \leq \sum_{(j, \beta) \in \delta_0^-(i, \alpha)} \tilde{a}_{i\alpha j\beta} \quad \forall \alpha \in N_i, \forall i \in V_c \quad (14)$$

Non-Overlapping Visits. When $y_{i(\alpha+1)} = 1$ and the node $(i, \alpha + 1)$ is visited, that is, customer i is visited for the $(\alpha + 1)^{\text{th}}$ time, then this customer must have been visited before, i.e., $y_{i\alpha} = 1$, as achieved by (15). Furthermore, constraints (16) require that the recent arrival must happen after the previous departure, since a customer is not allowed to be visited by more than one vehicle at the same time.

$$y_{i(\alpha+1)} \leq y_{i\alpha} \quad \forall \alpha \in N_i \setminus \{n_i\}, \forall i \in V_c \quad (15)$$

$$d_{i\alpha} \leq a_{i(\alpha+1)} + (H - t_{i0})(y_{i\alpha} - y_{i\alpha+1}) \quad \forall \alpha \in N_i \setminus \{n_i\}, \forall i \in V_c \quad (16)$$

Loading and Unloading Quantities. To model the loading and unloading quantities, we define the following continuous variables: $f_{i\alpha j\beta}$ denotes the amount of product that a vehicle transports from node (i, α) to node (j, β) in mode 0; $\ell_{j\beta}$ represents the amount of product that a vehicle, after finishing its current trip, reloads at the depot before immediately proceeding to node (j, β) ; and $q_{j\beta}$ is the total amount of product delivered to customer j at the β^{th} visit. We remark that $q_{j\beta}$ might be larger than $I_i^u - I_i^\ell$, since vehicles are allowed to remain at a customer location and dispense product multiple times before their departure. Constraints (20) require that any vehicle that travels from node (i, α) back to the depot is empty, while constraints (21) and (22) require that the vehicle capacity is respected. Constraints (23) impose upper limits on the unloading quantities,

while constraints (24) are the flow conservation constraints at node (j, β) , ensuring that the amount of product that flows into node (j, β) equals the delivered amount plus the amount that flows out.

$$f_{i\alpha j\beta} \in \mathbb{R}_+ \quad \forall (i, \alpha, j, \beta) \in A^0 : j \in V_c \quad (17)$$

$$\ell_{j\beta} \in \mathbb{R}_+ \quad \beta \in N_j, \forall j \in V_c \quad (18)$$

$$q_{j\beta} \in \mathbb{R}_+ \quad \beta \in N_j, \forall j \in V_c \quad (19)$$

$$f_{i\alpha 01} = 0 \quad \forall (i, \alpha) \in \delta_0^+(0, 1) \quad (20)$$

$$f_{i\alpha j\beta} \leq Q x_{i\alpha j\beta}^0 \quad \forall (i, \alpha, j, \beta) \in A^0 : j \in V_c \quad (21)$$

$$\ell_{j\beta} \leq Q \sum_{(i, \alpha) \in \delta_1^+(j, \beta)} x_{i\alpha j\beta}^1 \quad \forall \beta \in N_j, \forall j \in V_c \quad (22)$$

$$q_{j\beta} \leq Q y_{j\beta} \quad \forall \beta \in N_j, \forall j \in V_c \quad (23)$$

$$\sum_{(i, \alpha) \in \delta_0^+(j, \beta)} f_{i\alpha j\beta} + \ell_{j\beta} = q_{j\beta} + \sum_{(i, \alpha) \in \delta_0^-(j, \beta)} f_{j\beta i\alpha} \quad \forall \beta \in N_j, \forall j \in V_c \quad (24)$$

Inventory Limits. Inventory limits have to be respected for each customer at any moment in the continuous planning horizon. In order to achieve this, we specifically need to guarantee that, at the moment $a_{i\alpha}$ when a vehicle is arriving at customer $i \in V_c$, the inventory level is above the minimum desired level, I_i^ℓ , and that at the moment $d_{i\alpha}$ when a vehicle is departing from customer i , the inventory level is below the maximum level I_i^u , as enforced by constraints (25) and (26). Note that, during the time $[a_{i\alpha}, d_{i\alpha}]$, the vehicle remains at customer i and can perform multiple deliveries at zero extra cost, and thus the inventory limits I_i^ℓ and I_i^u will never be violated in that timeframe. At the end of the planning horizon, the inventory level at customer $i \in V_c$ should be above the target level I_i^H , as shown by (27).

$$I_i^0 y_{i\alpha} + \sum_{\substack{\alpha' \in N_i: \\ \alpha' < \alpha}} q_{i\alpha'} - r_i a_{i\alpha} \geq I_i^\ell y_{i\alpha} \quad \forall \alpha \in N_i, \forall i \in V_c \quad (25)$$

$$I_i^0 y_{i\alpha} + \sum_{\substack{\alpha' \in N_i: \\ \alpha' \leq \alpha}} q_{i\alpha'} - r_i d_{i\alpha} \leq I_i^u y_{i\alpha} + \sum_{\substack{\alpha' \in N_i: \\ \alpha' < \alpha}} Q (y_{i\alpha'} - y_{i\alpha}) \quad \forall \alpha \in N_i, \forall i \in V_c \quad (26)$$

$$I_i^0 + \sum_{\alpha \in N_i} q_{i\alpha} - r_i H \geq I_i^H \quad \forall i \in V_c \quad (27)$$

The CIRP aims to minimize the objective (1), subject to constraints (2)–(27). We highlight that this is a compact MILP formulation that can handle the complex routing and scheduling features

of the CIRP, such as multiple customer visits, multiple trips by a vehicle, and continuous-time inventory management.

4 Model Tightening

In this section, we derive various tightening inequalities to strengthen the LP relaxations of our proposed model. In particular, we tighten time windows of any visit to a customer and use them to eliminate variables from our proposed MILP formulation. We then consider the minimum quantity of product delivered to a customer and propose capacity constraints as strengthening cuts.

4.1 Tightening of Time Windows

We can tighten the time windows $[W_{j\beta}^\ell, W_{j\beta}^u]$ by taking advantage of the inventory restrictions. For example, the latest time point at which node (j, β) can be visited is when the inventory level at customer j , after a postulated $\beta - 1$ previous full truckload deliveries, reaches the minimum required level I_j^ℓ , namely the time $(I_j^0 + (\beta - 1)Q - I_j^\ell)/r_j$. Using similar reasoning, the node (j, β) cannot be visited too early, such that even if the inventory tops off during this visit and even if an additional $n_j - \beta$ full truckload deliveries are performed at a later time, the final inventory level is still above I_i^H at the end of the planning horizon. Hence, we may use the following tight values:

$$W_{j\beta}^\ell := \max \left\{ t_{0j}, H - \frac{I_j^u + (n_j - \beta)Q - I_j^H}{r_j} \right\},$$

$$W_{j\beta}^u := \min \left\{ H - t_{j0}, \frac{I_j^0 + (\beta - 1)Q - I_j^\ell}{r_j} \right\}.$$

We remark that one may further tighten these values by applying classical data preprocessing procedures as proposed in Kallehauge et al. (2007), noting though that we did not find this to be very beneficial in our computational studies.

4.2 Variable Elimination

Given node (i, α) , node (j, β) , and mode $d \in D$, whenever $W_{i\alpha}^\ell + T_{ij}^d > W_{j\beta}^u$, then we can fix $x_{i\alpha j\beta}^d = 0$. This represents a case where a vehicle cannot arrive at node (j, β) by the end of the applicable time window even if it departs node (i, α) at the earliest possible time.

Moreover, let us define $\vartheta_i := I_j^H + r_j H - I_j^0$ for each customer $i \in V_c$ to signify the minimum amount of product that the distributor has to ship to customer i during the planning horizon. Note how this amount barely guarantees that the inventory level is above I_i^H at the end of this horizon. We denote by m_i the minimum number of visits at customer i that have to be performed. Clearly, $m_i = \lceil \vartheta_i / Q \rceil$ since at most a full truckload (quantity Q) can be delivered to customer i in each visit. Hence, constraints (28) are valid. Then, for such nodes (i, α) that have to be visited in every feasible solution, we can enforce valid lower bounds for arrival time variables $a_{i\alpha}$, as shown by constraints (29).

$$y_{i\alpha} = 1 \quad \forall \alpha \in N_i : \alpha \leq m_i, \forall i \in V_c \quad (28)$$

$$a_{i\alpha} \geq W_{i\alpha}^\ell \quad \forall \alpha \in N_i : \alpha \leq m_i, \forall i \in V_c \quad (29)$$

4.3 Rounded Capacity Inequalities

The *rounded capacity inequalities* (Laporte and Nobert, 1983) are a well-known family of strengthening inequalities that have demonstrated great effectiveness in tightening routing models and expediting their solution process within a branch-and-cut framework (Toth and Vigo, 2002), among others. We adapt these inequalities to the context of the CIRP, yielding constraints

$$\sum_{j \in S} \sum_{\beta \in N_j} \left(\sum_{\substack{(i, \alpha) \in \delta_0^+(j, \beta): \\ i \notin S}} x_{i\alpha j\beta}^0 + \sum_{(i, \alpha) \in \delta_1^+(j, \beta)} x_{i\alpha j\beta}^1 \right) \geq k(S) \quad \forall S \subseteq V_c, \quad (30)$$

where $S \subseteq V_c$ denotes any subset of customers and $k(S)$ denotes the minimum number of vehicles required to serve the customers in S .

Note how the left-hand side in (30) represents the number of vehicles that are going to deliver product to customers in the set S , with the second term accounting for the case when vehicles return back to the depot for replenishment and then immediately serve customers in the set S . In regards to the right-hand side, $k(S)$ corresponds to the optimal value of the *bin-packing problem with item fragmentation* (Menakerman and Rom, 2001) (BPPIF) with bin capacity Q , item sizes given by the minimum demands (i.e., ϑ_i) of the customers in S , and each item fragmented into at most n_i pieces. Recognizing that computing this optimal value exactly is as hard as the BPPIF and is therefore strongly \mathcal{NP} -hard, the inequality remains valid if one replaces it with the obvious lower bound $k(S) := \lceil \sum_{i \in S} \vartheta_i / Q \rceil$, which yields the so-called *rounded capacity inequalities* (RCI).

We remark that capacity constraints similar to (30) are also used in the *vehicle routing problem with split delivery* (Belenguer et al., 2000; Bianchessi and Irnich, 2019).

In the spirit of a branch-and-cut algorithm, the polynomially-sized mixed-integer linear program (1)–(29) and (31) shall be initially presented to an MILP solver, while the RCI (30) will be dynamically separated and added into the model at each branch-and-bound node. In order to separate the above RCI, we first construct the support graph $\bar{G} = (V, E)$ that corresponds to the LP fractional solution at a given branch-and-bound node. In particular, we loop through all positive $\bar{x}_{i\alpha j\beta}^d$ values for $(i, \alpha, j, \beta) \in A^d, d \in D$, and we increment the weight of arc $(i, j) \in E$ by $\bar{x}_{i\alpha j\beta}^d$, if $d = 0$, while we increment the weights of both arcs $(i, 0) \in E$ and $(0, j) \in E$ by $\bar{x}_{i\alpha j\beta}^d$, if $d = 1$. We emphasize that the resulting graph \bar{G} is not the support graph that arises from the classic *capacitated vehicle routing problem* because the degree of each customer node is not necessarily exactly 2. Hence, the commonly used CVRPSEP package (Lysgaard, 2003) is not applicable here. Following a separation protocol similar to the one suggested in Lysgaard et al. (2004), we implemented three heuristics to separate our RCI, as follows. We first identify all *connected components* in the graph \bar{G} as candidates. Then, we separate the weaker *fractional capacity inequalities* via the max-flow algorithm. If both heuristics fail, we then resort to a custom-built variant of the *tabu search* method proposed by Augerat et al. (1998) to identify violated RCI.

A special case of (30) is when $S = V_c$, as shown by constraint (31). We notice that adding this constraint generally expedites the branch-and-cut algorithm; thus, in our implementation, we always append this one to our formulation from the onset.

$$\sum_{j \in V_c} \sum_{\beta \in N_j} \left(x_{01j\beta}^0 + \sum_{(i, \alpha) \in \delta_1^+(j, \beta)} x_{i\alpha j\beta}^1 \right) \geq \left\lceil \frac{\sum_{i \in V_c} \vartheta_i}{Q} \right\rceil \quad (31)$$

5 Computational Studies

In this section, we test our branch-and-cut algorithm on CIRP benchmark instances and compare it against the state-of-the-art approach from Lagos et al. (2020). Our algorithm was implemented in C++ and the mixed-integer linear program was solved using the Gurobi Optimizer 10.0.1 through the C application programming interface. User cuts were implemented via the Gurobi callback function, while branching prioritized binary variables $y_{i\alpha}$ before considering $x_{i\alpha j\beta}^d$ variables. All solver settings were kept at their default, except the optimality gap tolerances, with the relative

tolerance set to 0 (effectively disabled) and the absolute one to the value of 0.0099. Note that the latter suffices for any optimal solutions to be exact, since all entries of the travel cost matrix in all datasets used have at most two decimal digits and, hence, so does the objective value of any feasible solution. All computations were performed on a server with dual Intel Xeon E5-2689v4 CPUs clocking at 3.10 GHz. The 128 GB of available RAM was shared among 10 copies of the algorithm running in parallel on this machine. Each instance was solved by one copy of the algorithm limited to use a single thread.

5.1 Benchmark Instances

We consider two CIRP datasets for testing our algorithm. The first one stems from the work of Lagos et al. (2020), in which the authors generated two types of CIRP instances, namely **clustered** (C) and **random** (R). There are 45 instances for each type, with the number of customers ranging from 5 to 15 and the number of vehicle ranging from 3 to 15. All instances can be found at <https://github.com/felipelagos/cirplib>. As per Lagos et al. (2020), the travel costs and travel times are taken as the Euclidean distances rounded to two decimal places.

Furthermore, to evaluate the performance of our algorithm on solving realistic CIRP data, we generate another dataset that is inspired by the ROADEF/EURO Challenge 2016 competition (ROADEF, 2016). In particular, we obtain the “version 1.1 set A” dataset from this competition and apply the following modifications: (i) the fleet is reduced to a homogeneous one; (ii) the driver-trailer scheduling aspect is neglected; (iii) the product consumption rate is considered to be constant throughout the planning horizon; (iv) the objective is to minimize the travel cost, rather than the logistic ratio. We highlight that this dataset includes 9 medium-size instances stemming from real-life practice, with the number of customers ranging from 53 to 89. To create our CIRP instances, we choose the first 5, 7, 10, 12, 15, 17 and 20 customers from each original instance, thus resulting in a suite of 63 instances that we shall refer to as the **roadef** (RF) type. The number of vehicles in our instances ranges from 1 to 6. Our newly generated instances are named “RF-X-nY-kZ” to signify how the X^{th} original instance was adapted to include Y customers and Z vehicles. All instance data can be found at <http://gounaris.cheme.cmu.edu/datasets/cirp/>.

In all our experiments, we limit the number of visits to each customer $i \in V_c$ to two plus the minimal number of visits at customer i , i.e., $n_i := m_i + 2$, since we did not notice any improvement

in the optimal objective values when we increase this number.

5.2 Computational Results on Literature Benchmarks

We first test our branch-and-cut algorithm (denoted by “Branch-and-Cut”) on the first dataset (clustered and random instances) and compare its performance with that from the work of Lagos et al. (2020) (denoted by LBS20). To analyze the effect of adding RCI on the solution process, we consider a variant of our algorithm in which RCI are disabled. In this case, no user cuts are added to the model and hence we denote it by “Gurobi (default)”. We also highlight that, in the “Branch-and-Cut” approach, all Gurobi-generated, general-purpose cuts were disabled because we observed that using them decreased overall computational performance.

We impose a time limit of 10 hours for each instance and compare our computational results with those from LBS20 in Table 1. Columns “# cust.” and “# inst.” report the number of customers in an instance and the number of instances of such an input size, respectively. For each respective algorithm, the column “# opt.” reports the number of instances that were solved to optimality within the time limit, while column “# t.l.” reports the number of instances for which the algorithm was terminated due to the time limit but with valid lower and upper bounds identified. For the instances solved to optimality, we report the average solution time (in seconds, rounded to the nearest integer) in column “Avg. t (s)”. For the unsolved instances, we report in column “Avg. gap (%)” the average residual gap, defined as $(UB - LB)/UB$ at the time limit. Note that Table 1 does not present solution times for the LBS20 algorithm since, in their adopted approach, the authors solve a sequence of parametric MILPs for which cumulative solution times were not reported.

Out of the totality of 90 CIRP instances, LBS20 solved 26 of them to optimality, returning an average residual gap of 6.45% in the remaining 64. In contrast, the proposed “Branch-and-Cut” algorithm solved 57 instances to guaranteed optimality with an average gap of 1.25% for the remaining 33. In particular, our algorithm solved to optimality all 5- and 7-customer instances, approximately half of 10-customer ones, as well as a few of the 12- and 15-customer instances. Addressing the CIRP using the “Gurobi (default)” approach was found to be moderately effective, being able to prove optimality for 42 instances, while returning an average residual gap of 3.85% for the remaining ones. It is noteworthy that a practitioner can readily take advantage of this latter

approach’s performance, since it merely calls for implementing and solving our formulation as a monolithic MILP model, without incorporating the cut separation routine.

Tables 2 and 3 present detailed results on the **clustered** (C) and **random** (R) instances, respectively, for our proposed “Branch-and-Cut” algorithm. In these tables, if an instance could be solved to optimality within 10 hours, then “Opt [UB]” reports the corresponding optimal objective value, while “t (s) [LB]” reports the time (in seconds, rounded to the nearest integer) to solve the instance to optimality. Otherwise, the columns respectively report in brackets the best upper and lower bounds found by the time limit. We also report the average number of visits across all customers in the returned best known solution to each instance (column “Avg. # visits”) and the number of RCI that have been dynamically added (column “# RCI”). Notably, the average number of visits to every customer ranges from 1.2 to 2.2, which is far from the maximum number of allowable visits, n_i , which generally ranges from 3 to 5. This indicates that our choice of the number of allowable visits is not restrictive.

We now revisit Table 1 for evaluating the effect of RCI on the branch-and-bound process. Compared with the “Gurobi (default)” version, the “Branch-and-Cut” algorithm with RCI enabled as strengthening inequalities solved to optimality 15 additional benchmark instances, including a few of the larger 15-customer ones. We also note that solution times and residual gaps for unsolved instances were decreased across the board, indicating the effectiveness of RCI in expediting the branch-and-bound based search process. To better illustrate this, performance profiles (Dolan and Moré, 2002) are presented in Figure 1. Finally, it is worthy to note that the total number of RCI that were identified and introduced as tightening inequalities is in the order of hundreds for small-sized CIRP instances, increasing to tens of thousands for the large-sized ones (see Tables 2 and 3).

5.3 Computational Results on roadef Instances

We now turn our attention to the set of the newly constructed **roadef** instances and evaluate the performance of the “Branch-and-Cut” algorithm on those. The imposed time limit was again chosen as 10 hours. A synopsis of our computational results is presented in Table 4 while the detailed results are reported in Table 5. Out of the 63 instances in this dataset, our “Branch-and-Cut” algorithm solved 58 to optimality and returned an average residual gap of 0.11% for the remaining

Table 1. Comparison among LBS20 and our proposed approaches on benchmark instances

# cust. # inst.		LBS20			Gurobi (default)				Branch-and-Cut				
		# opt.	# t.l.	Avg.	# opt.	# t.l.	Avg. t	Avg.	# opt.	# t.l.	Avg. t	Avg.	
				gap (%)			(s)	gap (%)			(s)	gap (%)	
clustered													
5	9	7	2	1.55	9	0	12	–	9	0	1	–	
7	9	3	6	1.92	9	0	6,335	–	9	0	4,043	–	
10	9	1	8	1.90	2	7	14,211	2.22	4	5	8,176	1.14	
12	9	1	8	3.26	0	9	–	3.59	2	7	72	0.85	
15	9	1	8	8.55	0	9	–	6.03	1	8	92	1.18	
random													
5	9	5	4	2.93	9	0	2	–	9	0	1	–	
7	9	5	4	3.27	8	1	143	2.32	9	0	21	–	
10	9	3	6	4.10	4	5	1,891	1.48	7	2	105	1.98	
12	9	0	9	8.93	1	8	2,179	2.95	5	4	3,164	2.02	
15	9	0	9	17.67	0	9	–	5.48	2	7	3,528	1.14	
Total	90	26	64		42	48			57	33			
Avg.				6.45			2,297	3.85			1,634	1.25	

Table 2. Detailed results for the Branch-and-Cut algorithm on 45 **clustered** instances

Inst.	Opt [UB]	t (s) [LB]	Avg. # visits	# RCI	Inst.	Opt [UB]	t (s) [LB]	Avg. # visits	# RCI
C5U1Q1	37.85	1	1.4	2	C10U2Q3	[55.96]	[54.87]	1.8	163,551
C5U1Q2	30.61	1	1.4	8	C10U3Q1	104.37	2,232	2.1	721
C5U1Q3	28.24	1	1.2	6	C10U3Q2	[83.36]	[83.17]	1.9	173,689
C5U2Q1	50.09	1	1.8	8	C10U3Q3	[65.62]	[64.91]	1.7	93,896
C5U2Q2	38.28	2	1.6	25	C12U1Q1	85.07	7	1.5	30
C5U2Q3	30.61	1	1.4	13	C12U1Q2	[69.28]	[68.82]	1.6	99,696
C5U3Q1	57.74	7	2.2	83	C12U1Q3	[57.07]	[56.49]	1.6	218,045
C5U3Q2	43.36	1	1.8	10	C12U2Q1	[104.29]	[104.11]	2.0	8,850
C5U3Q3	36.16	1	1.8	8	C12U2Q2	[80.01]	[79.28]	1.8	133,401
C7U1Q1	52.14	1,683	1.7	3,277	C12U2Q3	[69.49]	[68.85]	1.7	175,158
C7U1Q2	42.99	11,932	1.7	76,645	C12U3Q1	124.43	137	2.1	76
C7U1Q3	31.17	24	1.4	58	C12U3Q2	[101.72]	[101.06]	2.0	89,840
C7U2Q1	59.75	5	1.9	36	C12U3Q3	[80.22]	[78.92]	1.8	51,573
C7U2Q2	50.48	15,371	2.0	54,943	C15U1Q1	99.78	92	1.5	213
C7U2Q3	42.18	43	1.6	188	C15U1Q2	[77.32]	[76.59]	1.5	33,244
C7U3Q1	78.08	3	2.1	25	C15U1Q3	[64.53]	[63.92]	1.5	111,357
C7U3Q2	59.44	5	1.6	29	C15U2Q1	[122.67]	[122.06]	1.9	12,877
C7U3Q3	50.18	7,325	1.7	10,265	C15U2Q2	[94.97]	[93.98]	1.8	10,074
C10U1Q1	70.97	17	1.4	109	C15U2Q3	[78.88]	[76.60]	1.7	38,569
C10U1Q2	[55.64]	[54.86]	1.6	229,417	C15U3Q1	[147.06]	[147.02]	2.1	428
C10U1Q3	45.24	27,412	1.5	189,524	C15U3Q2	[118.72]	[116.43]	2.1	52,311
C10U2Q1	86.02	3,044	1.8	229	C15U3Q3	[94.67]	[93.58]	1.9	23,454
C10U2Q2	[65.92]	[65.24]	1.8	269,768					

Table 3. Detailed results for the Branch-and-Cut algorithm on 45 **random** instances

Inst.	Opt [UB]	t (s) [LB]	Avg. # visits	# RCI	Inst.	Opt [UB]	t (s) [LB]	Avg. # visits	# RCI
R5U1Q1	36.42	1	1.4	2	R10U2Q3	64.02	10	1.5	64
R5U1Q2	29.06	1	1.2	3	R10U3Q1	116.04	179	2.3	252
R5U1Q3	28.45	1	1.2	13	R10U3Q2	[93.93]	[92.18]	2.0	90,149
R5U2Q1	41.42	1	1.8	7	R10U3Q3	82.92	120	1.8	292
R5U2Q2	36.51	1	1.6	11	R12U1Q1	[101.88]	[99.90]	1.8	88,146
R5U2Q3	30.90	1	1.4	9	R12U1Q2	75.45	43	1.5	144
R5U3Q1	45.31	1	2.0	8	R12U1Q3	66.09	13,637	1.2	43,893
R5U3Q2	39.44	3	2.0	9	R12U2Q1	[118.75]	[118.48]	2.0	4,667
R5U3Q3	33.54	2	1.6	33	R12U2Q2	98.18	136	1.8	419
R7U1Q1	63.03	1	1.6	82	R12U2Q3	76.27	1,888	1.5	2,226
R7U1Q2	43.93	1	1.3	16	R12U3Q1	139.88	118	2.1	141
R7U1Q3	40.43	146	1.6	773	R12U3Q2	[111.63]	[107.60]	1.8	63,004
R7U2Q1	69.37	1	1.7	16	R12U3Q3	[95.74]	[93.53]	1.8	116,905
R7U2Q2	60.12	1	1.7	10	R15U1Q1	[117.71]	[117.53]	1.8	17,975
R7U2Q3	43.93	2	1.3	34	R15U1Q2	87.67	4,371	1.7	1,163
R7U3Q1	81.58	2	2.0	15	R15U1Q3	75.25	2,685	1.3	6,034
R7U3Q2	67.06	2	2.0	18	R15U2Q1	[139.63]	[138.72]	1.9	110,116
R7U3Q3	57.47	32	1.9	143	R15U2Q2	[118.39]	[114.43]	1.9	166,367
R10U1Q1	[87.72]	[85.88]	1.9	95,209	R15U2Q3	[89.45]	[88.72]	1.6	58,087
R10U1Q2	64.02	6	1.5	53	R15U3Q1	[162.61]	[161.98]	2.1	3,327
R10U1Q3	54.35	305	1.2	1,126	R15U3Q2	[128.52]	[127.75]	1.9	50,005
R10U2Q1	99.48	2	1.9	37	R15U3Q3	[113.37]	[111.08]	1.7	148,586
R10U2Q2	82.92	112	1.8	134					

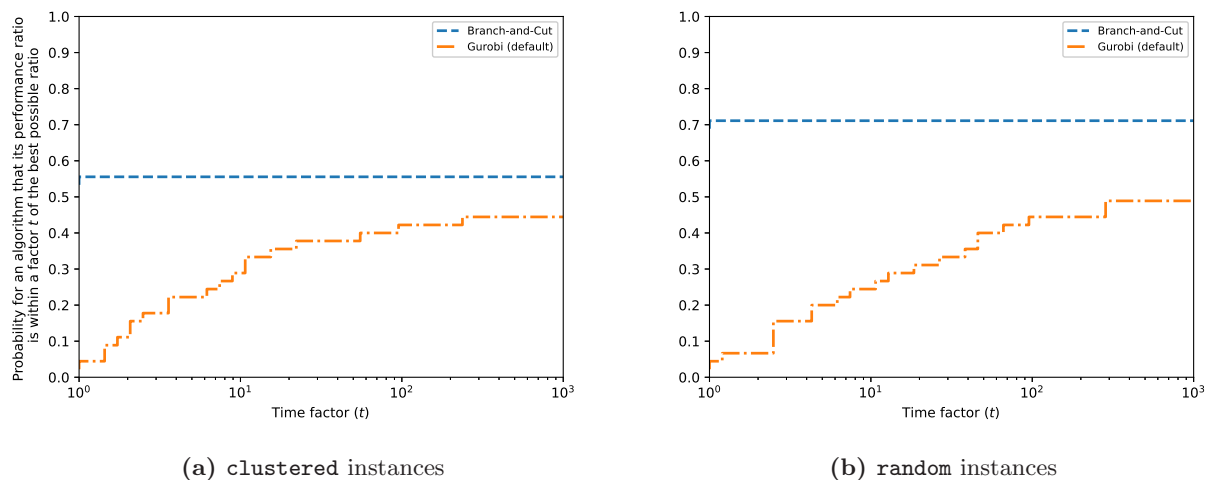


Figure 1. Log-scaled performance profiles across all benchmark instances. For each curve, the value at $t = 0$ indicates the fraction of benchmark instances that can be solved the fastest via the corresponding approach, while the limiting value at $t \rightarrow \infty$ indicates the fraction of instances that could be solved within the time limit.

5 instances. In particular, our algorithm solved all instances with up to 10 customers as well as the vast majority of the larger ones with up to 20 customers. Notably, our approach was able to identify feasible solutions in all instances. The solution times generally increase with problem size, ranging from minutes to a few hours. Interestingly, the average customer is visited several times (about 3) during the planning horizon. Here, we should point out that the “Gurobi (default)” approach was again outperformed by our “Branch-and-Cut” approach. For reference, the former could solve to optimality only 18 of these `roadef` instances within the same time limit. For the sake of brevity, we omit presenting the detailed computational results for that method.

6 Conclusions

In this work, we consider the continuous-time inventory routing problem (IRP), a challenging setting with ubiquitous practical application. This problem often arises in the context of vendor-managed inventory systems where the distributor monitors the customer’s product usage and is charged with actively managing inventory levels at the customer site. Notably, the level of the inventory must be maintained within acceptable limits in continuous time, unlike earlier IRP models that only

Table 4. Results synopsis for the Branch-and-Cut algorithm on **roadef** instances

# cust.	# inst.	# opt.	# t.l.	Avg. t (s)	Avg. gap (%)	Avg. # visits
5	9	9	0	39	–	2.7
7	9	9	0	957	–	2.7
10	9	9	0	1,144	–	3.0
12	9	8	1	5,605	0.09	3.0
15	9	8	1	2,325	0.12	2.8
17	9	8	1	4,195	0.05	2.9
20	9	7	2	13,142	0.15	2.7
Total	63	58	5			
Avg.				3,591	0.11	2.8

enforced this in discrete time points during the planning horizon.

We propose a novel mixed-integer linear programming formulation that incorporates multi-trip and multi-visit features as well as continuous-time inventory management. To expedite the solution process, we propose various types of tightening techniques, including among others the adaptation of well-known rounded capacities inequalities. We conduct extensive computational studies on 90 benchmark instances from the literature, revealing the effectiveness of our branch-and-cut algorithm and its outperforming of the previous state-of-the-art approach. In particular, we close 30 previously open CIRP benchmark instances and return an average gap below 2% for the unsolved instances. We also further computational studies using newly constructed benchmarks based on real-life data. These show that our proposed algorithm could solve CIRP instances of up to 20 customers and 6 vehicles.

Overall, the CIRP constitutes an extremely challenging problem, especially as one compares with its discrete-time IRP counterpart for which state-of-the-art approaches can address instances with up to 100 customers. It remains a question for the practitioner whether the more rigorous feasibility guarantees afforded by tracking and enforcing inventory limits in continuous time are worth the associated tractability hit.

Table 5. Detailed results for the Branch-and-Cut algorithm on 63 `roadef` instances

Inst.	Opt [UB]	t (s) [LB]	Inst.	Opt [UB]	t (s) [LB]	Inst.	Opt [UB]	t (s) [LB]
RF-3-n5-k1	1,043.7	1	RF-6-n10-k3	1,998.9	1,721	RF-9-n15-k3	2,000.7	3,647
RF-4-n5-k1	1,043.7	1	RF-7-n10-k1	1,652.4	4808	RF-10-n15-k2	2,520.0	1,354
RF-5-n5-k1	566.1	1	RF-8-n10-k2	1,837.5	678	RF-11-n15-k3	2,520.0	300
RF-6-n5-k1	572.4	1	RF-9-n10-k2	1,631.1	798	RF-3-n17-k3	4,886.0	1,512
RF-7-n5-k1	492.0	6	RF-10-n10-k2	1,869.6	63	RF-4-n17-k2	4,603.2	2,291
RF-8-n5-k1	524.7	178	RF-11-n10-k2	1,869.6	130	RF-5-n17-k4	[2,305.8]	[2,304.6]
RF-9-n5-k1	480.6	140	RF-3-n12-k2	3,804.5	24,891	RF-6-n17-k5	2,421.9	1,232
RF-10-n5-k1	1,323.9	8	RF-4-n12-k2	3,757.6	1,901	RF-7-n17-k3	2,094.0	4,821
RF-11-n5-k1	1,323.9	20	RF-5-n12-k4	[2,034.9]	[2,033.1]	RF-8-n17-k4	2,366.1	5,262
RF-1-n7-k2	6,318.0	12	RF-6-n12-k3	2,157.6	2,997	RF-9-n17-k3	2,050.8	7,992
RF-2-n7-k2	6,309.0	8	RF-7-n12-k2	1,760.7	320	RF-10-n17-k4	3,145.8	2,238
RF-3-n7-k2	2,618.7	87	RF-8-n12-k2	1,945.8	7,056	RF-11-n17-k4	3,173.7	8,211
RF-4-n7-k1	2,618.7	3,846	RF-9-n12-k2	1,739.4	748	RF-3-n20-k4	5,518.8	9,145
RF-5-n7-k2	927.3	6	RF-10-n12-k2	1,996.5	950	RF-4-n20-k3	7,410.2	22,482
RF-6-n7-k1	1,007.1	24	RF-11-n12-k2	1,996.5	5,976	RF-5-n20-k4	[2,315.4]	[2,313.9]
RF-7-n7-k1	739.8	3,321	RF-3-n15-k2	4,552.8	735	RF-6-n20-k4	2,435.7	8,505
RF-8-n7-k1	781.5	205	RF-4-n15-k3	4,027.8	121	RF-7-n20-k4	2,306.4	7,698
RF-9-n7-k1	731.7	1,104	RF-5-n15-k4	[2,277.3]	[2,274.6]	RF-8-n20-k6	[2,583.0]	[2,577.0]
RF-3-n10-k2	3,086.3	176	RF-6-n15-k1	2,392.8	1,947	RF-9-n20-k4	2,280.0	3,194
RF-4-n10-k1	2,913.4	1,707	RF-7-n15-k2	2,052.6	9,081	RF-10-n20-k4	3,375.6	5,862
RF-5-n10-k3	1,879.8	209	RF-8-n15-k3	2,314.2	1,413	RF-11-n20-k4	3,427.5	35,112

Acknowledgments

We acknowledge financial support from Air Liquide through the Center for Advanced Process Decision-making (CAPD) at Carnegie Mellon University. Akang Wang also greatly acknowledges support from the James C. Meade Graduate Fellowship and the H. William and Ruth Hamilton Prengle Graduate Fellowship at Carnegie Mellon University.

References

- Absi, N., Cattaruzza, D., Feillet, D., Ogier, M., and Semet, F. (2020). A heuristic branch-cut-and-price algorithm for the roadeff/euro challenge on inventory routing. *Transportation Science*, 54(2):313–329.
- Agra, A., Christiansen, M., Hvattum, L. M., and Rodrigues, F. (2018). Robust optimization for a maritime inventory routing problem. *Transportation Science*, 52(3):509–525.
- Agra, A., Christiansen, M., and Wolsey, L. (2022). Improved models for a single vehicle continuous-time inventory routing problem with pickups and deliveries. *European Journal of Operational Research*, 297(1):164–179.
- Arbogast, J. E. and Kontopoulos, A. (2017). Air Liquide: Multinational company’s computational and data science R & D team supports an extensive, varied, dynamic research portfolio. *OR/MS Today*, pages 18–21.
- Archetti, C., Bertazzi, L., Laporte, G., and Speranza, M. G. (2007). A branch-and-cut algorithm for a vendor-managed inventory-routing problem. *Transportation science*, 41(3):382–391.
- Archetti, C., Desaulniers, G., and Speranza, M. G. (2017). Minimizing the logistic ratio in the inventory routing problem. *EURO Journal on Transportation and Logistics*, 6(4):289–306.
- Augerat, P., Belenguer, J.-M., Benavent, E., Corb  ran, A., and Naddef, D. (1998). Separating capacity constraints in the cvrp using tabu search. *European Journal of Operational Research*, 106(2-3):546–557.
- Avella, P., Boccia, M., and Wolsey, L. A. (2017). Single-period cutting planes for inventory routing problems. *Transportation Science*, 52(3):497–508.

- Baldacci, R., Lim, A., Traversi, E., and Wolfler Calvo, R. (2020). Optimal solution of vehicle routing problems with fractional objective function. *Transportation Science*, 54(2):434–452.
- Belenguer, J.-M., Martinez, M., and Mota, E. (2000). A lower bound for the split delivery vehicle routing problem. *Operations Research*, 48(5):801–810.
- Bianchessi, N. and Irnich, S. (2019). Branch-and-cut for the split delivery vehicle routing problem with time windows. *Transportation Science*, 53(2):442–462.
- Coelho, L. C., Cordeau, J.-F., and Laporte, G. (2012). Consistency in multi-vehicle inventory-routing. *Transportation Research Part C: Emerging Technologies*, 24:270–287.
- Coelho, L. C., Cordeau, J.-F., and Laporte, G. (2013). Thirty years of inventory routing. *Transportation Science*, 48(1):1–19.
- Coelho, L. C. and Laporte, G. (2013). The exact solution of several classes of inventory-routing problems. *Computers & Operations Research*, 40(2):558–565.
- Coelho, L. C. and Laporte, G. (2014). Improved solutions for inventory-routing problems through valid inequalities and input ordering. *International Journal of Production Economics*, 155:391–397.
- Desaulniers, G., Rakke, J. G., and Coelho, L. C. (2015). A branch-price-and-cut algorithm for the inventory-routing problem. *Transportation Science*, 50(3):1060–1076.
- Dolan, E. D. and Moré, J. J. (2002). Benchmarking optimization software with performance profiles. *Mathematical Programming*, 91(2):201–213.
- Dong, Y., Maravelias, C. T., Pinto, J. M., and Sundaramoorthy, A. (2017). Solution methods for vehicle-based inventory routing problems. *Computers & Chemical Engineering*, 101:259–278.
- Fokkema, J. E., Land, M. J., Coelho, L. C., Wortmann, H., and Huitema, G. B. (2020). A continuous-time supply-driven inventory-constrained routing problem. *Omega*, 92:102151.
- He, Y., Artigues, C., Briand, C., Jozefowicz, N., and Ngueveu, S. U. (2020). A matheuristic with fixed-sequence reoptimization for a real-life inventory routing problem. *Transportation Science*, 54(2):355–374.

- Kallehauge, B., Boland, N., and Madsen, O. B. (2007). Path inequalities for the vehicle routing problem with time windows. *Networks: An International Journal*, 49(4):273–293.
- Karaoglan, I. (2015). A branch-and-cut algorithm for the vehicle routing problem with multiple use of vehicles. *Int’l J. of Lean Thinking*, 6(1).
- Kheiri, A. (2020). Heuristic sequence selection for inventory routing problem. *Transportation Science*, 54(2):302–312.
- Koyuncu, I. and Yavuz, M. (2019). Duplicating nodes or arcs in green vehicle routing: A computational comparison of two formulations. *Transportation Research Part E: Logistics and Transportation Review*, 122:605–623.
- Lagos, F., Boland, N., and Savelsbergh, M. (2020). The continuous-time inventory-routing problem. *Transportation Science*, 54(2):375–399.
- Lagos, F., Boland, N., and Savelsbergh, M. (2022). Dynamic discretization discovery for solving the continuous time inventory routing problem with out-and-back routes. *Computers & Operations Research*, 141:105686.
- Laporte, G. and Nobert, Y. (1983). A branch and bound algorithm for the capacitated vehicle routing problem. *Operations-Research-Spektrum*, 5(2):77–85.
- Lysgaard, J. (2003). Cvrpsep: A package of separation routines for the capacitated vehicle routing problem.
- Lysgaard, J., Letchford, A. N., and Eglese, R. W. (2004). A new branch-and-cut algorithm for the capacitated vehicle routing problem. *Mathematical Programming*, 100(2):423–445.
- Menakerman, N. and Rom, R. (2001). Bin packing with item fragmentation. In *Workshop on Algorithms and Data Structures*, pages 313–324. Springer.
- Radzik, T. (2013). Fractional combinatorial optimization. *Handbook of combinatorial optimization*, pages 1311–1355.
- ROADEF (2016). <https://www.roadef.org/challenge/2016/en/index.php>.

- Rothenbächer, A.-K. (2019). Branch-and-price-and-cut for the periodic vehicle routing problem with flexible schedule structures. *Transportation Science*, 53(3):850–866.
- Singh, T., Arbogast, J. E., and Neagu, N. (2015). An incremental approach using local-search heuristic for inventory routing problem in industrial gases. *Computers & Chemical Engineering*, 80:199–210.
- Su, Z., Lü, Z., Wang, Z., Qi, Y., and Benlic, U. (2020). A matheuristic algorithm for the inventory routing problem. *Transportation Science*, 54(2):330–354.
- Toth, P. and Vigo, D. (2002). *The vehicle routing problem*. SIAM.
- Yao, Y., Evers, P. T., and Dresner, M. E. (2007). Supply chain integration in vendor-managed inventory. *Decision Support Systems*, 43(2):663–674.